Hypoxia modulates A431 cellular pathways association to tumor radioresistance and enhanced migration revealed by comprehensive proteomic and functional studies

Ren, Yan; Hao, Piliang; Dutta, Bamaprasad; Cheow, Esther Sok Hwee; Sim, Kae Hwan; Gan, Chee Sian; Lim, Sai Kiang; Sze, Siu Kwan

2013

Ren, Y., Hao, P., Dutta, B., Cheow, E. S. H., Sim, K. H., Gan, C. S., et al. (2013). Hypoxia modulates A431 cellular pathways association to tumor radioresistance and enhanced migration revealed by comprehensive proteomic and functional studies. Molecular and cellular proteomics, 12, 485-498.

https://hdl.handle.net/10356/96650

https://doi.org/10.1074/mcp.M112.018325

Hypoxia Modulates A431 Cellular Pathways Association to Tumor Radioresistance and Enhanced Migration Revealed by Comprehensive Proteomic and Functional Studies

Yan Ren[1], Piliang Hao[1], Bamaprasad Dutta[1], Esther Sok Hwee Cheow[1], Kae Hwan Sim[1], Chee Sian Gan[2], Sai Kiang Lim[3] and Siu Kwan Sze[1]*

1. School of Biological Sciences, Nanyang Technological University, 60 Nanyang Drive, Singapore 637551

2. Agilent Technologies, Inc.1 Yishun Avenue 7, Singapore 768923

3. Institute of Medical Biology, A*STAR, 8A Biomedical Grove, Immunos, Singapore 138648

Running title: Radioresistance and Migration of Hypoxic Tumor Cells

Correspondence:
Dr. Siu Kwan SZE Tel:
(+65)6514-1006 Fax:
(+65)6791-3856 Email:
sksze@ntu.edu.sg

Abbreviations

HIF-1, hypoxia-inducible factor-1; iTRAQ, isobaric tag for relative and absolute quantification; MRM, multiple reaction monitoring; TEAB, triethylammonium bicarbonate; MMTS, methyl methanethiosulfonate; FDR, false discovery rate; EF, error factor; PAGE, polyacrylamide gel electrophoresis; WB, Western blot; PCR, polymerase chain reaction; NHEJ, Nonhomologous end-joining; HR, homologous recombination; NHEJ1, Nonhomologous end-joining factor 1; 2-DG, 2-Deoxy-D-glucose; HIF-1, hypoxia-inducible factor-1; ECM, extracellular matrix; MMP, matrix metalloproteinase; 2-DE, Two-dimensional electrophoresis; DMEM, Dulbecco's modified Eagle's medium; FBS, fetal bovine serum; IPA, Ingenuity Pathway Analysis; DSB, DNA double strand break; TCA, tricarboxylic acid; Ku70, X-ray repair cross-complementing protein 6; Ku80, X-ray repair cross-complementing protein 5; STAT1, Signal transducer and activator of transcription 1; RAD51, DNA repair protein RAD51 homolog 1; BRCA1/2, breast cancer type 1/2 susceptibility protein; XRCC3/4, DNA repair protein XRCC3/4; SCX, Strong Cation Exchange; FA, formic acid; ITGB1, integrin beta 1; ITGA5, integrin alpha 5; LDHA, L-lactate dehydrogenase A chain; PDHB, Pyruvate dehydrogenase E1 component subunit beta; IFN, interferon; IRF-1, Interferon regulatory factor 1; PIAS1, E3 SUMO-protein ligase PIAS1; JNK/1/2, c-Jun N-terminal kinase1/2; The other abbreviations of proteins used in this article were listed in Supplemental Table S2.

Summary

Tumor hypoxia induces cancer cell angiogenesis, invasiveness, treatment resistance, and contributes to poor clinical outcome. However, the molecular mechanism by which tumor hypoxia exerted a coordinated effect on different molecular pathways to enhance tumor growth and survival and lead to poor clinical outcome is not fully understood. In this study, we attempt to elucidate the global protein expression and functional changes in A431 epithelial carcinoma cells induced by hypoxia and reoxygenation using iTRAQ quantitative proteomics and biochemical functional assays. Quantitative proteomics results showed that 4,316 proteins were quantified with FDR<1%, in which over 1,200 proteins were modulated >1.2 folds, and DNA repair, glycolysis, integrin, glycoprotein turnover and STAT1 pathways were perturbed by hypoxia and reoxygenation-induced oxidative stress. For the first time, hypoxia was shown to up-regulate the nonhomologous end-joining (NHEJ) pathway which plays a central role in DNA repair of irradiated cells, thereby potentially contributing to the radioresistance of hypoxic A431 cells. The up-regulation of Ku70/Ku80 dimer, a key molecular complex in the NHEJ pathway, was confirmed by WB and LC-MS/MS-MRM methods. Functional studies confirmed that up-regulation of glycolysis, integrin, glycoprotein synthesis and down-regulation of STAT1 pathways during hypoxia enhanced metastastic activity of A431 cells. Migration of A431 cells was dramatically repressed by glycolysis inhibitor (2-Deoxy-D-glucose), glycoprotein synthesis inhibitor (1-Deoxynojirimycin Hydrochloride), and STAT1a overexpression that enhanced the integrin-mediated cell adhesion. These results revealed that hypoxia induced several biological processes involved in tumor migration and radioresistance and provided potential new targets for tumor therapy.

Introduction

Tumor hypoxia arises when solid tumor expands too rapidly without a concomitant expansion of the supporting vasculature (1). Tumor hypoxia induces resistance to anti-cancer therapeutics, angiogenesis, genomic instability, invasion/metastasis and overall poor clinical outcome (2, 3). Given its importance in tumor development, the molecular pathways perturbed by tumor hypoxia are considered attractive targets to be exploited in oncology (4).

Extensive laboratory studies and clinical data have shown that hypoxic conditions contribute to therapeutic resistance in radiotherapy and limit the response of tumor cells to radiation therapy (5-7). DNA damage by irradiation is kept from repair with the presence of oxygen, but it can be repaired by hydrogen without oxygen under hypoxia and thus leads to increased radioresistance (7). Other biological molecules have also been reported to be involved in the radioresistance in tumor cells under hypoxic conditions (8). A major cellular response to hypoxia is the activation of hypoxia induced factor 1 (HIF-1), a transcription factor, which has been implicated in the regulation of tumor radiosensitivity (9). HIF-1a expression in uterine cervical cancer tissues positively correlates with the adverse effects of radiotherapy, and its expression in cervical cancer after radiotherapy is associated with increased risk for tumor-related death (10, 11). DNA repair pathways are vital for cellular protection against radiation. Recent studies showed that the activation of DNA repair pathways in some tumors contributed to intrinsic resistance to radiotherapy (12, 13). However, several reports have demonstrated that hypoxia induces the repression of DNA repairing genes at the mRNA level, for example, RAD51, BRCA1/2, XRCC3/4, Ku70 and Ligase IV, but the changes in mRNA level do not always correlate with a

subsequent decrease in protein level (14-17). These data thus highlight the importance of determining whether some of functional consequences of hypoxia were mediated by DNA repair proteins.

Laboratory and clinical studies have also indicated that tumor hypoxia has also been implicated in enhancing tumor cell metastatic potential (3, 18-22). Metastasis is the major characteristics of malignant tumors and the main cause for cancer-related mortalities. As such, there have been major efforts to elucidate the molecular mechanisms underlying the distinct steps of cancer metastasis (23-26). Some key molecules, such as adhesion molecules and MMPs, play important role in cancer cell metastasis(27). It was reported that HIF-1 modulates the expression level of proteins, such as MMPs, plasminogen activator inhibitor (PAI-1), tissue factors, CapG, S100A4, filamentation 1, cadherin and integrin alpha 5 (2, 28-30), which play important roles in regulating the invasion or metastatic potential of tumor cells.

Hypoxia is now a well recognized cause of radioresistance and metastasis but its precise role in these processes is still poorly defined (24, 31). A better understanding of the mechanisms behind this pathophysiology will lead to a more specific and efficient therapeutic outcome. The knowledge of hypoxia-regulated proteins from proteomic investigation will provide a better and global understanding of the molecular pathways perturbed by hypoxic tumour and give rise to novel biological insights and concepts for exploiting this factor (7).

Proteomic studies to elucidate the molecular events elicited by hypoxic stress (3, 3234) are less extensive and have, to date been limited to the use of 2-DE based methods (35). To further our proteomic knowledge of hypoxia-induced tumor evolution,

shotgun based iTRAQ quantitative proteomics, which provides a global assessment of the proteins modulated, was used to analyze the cellular proteome changes of A431 epithelial carcinoma cells induced by hypoxia and reoxygenation. More than 4,300 proteins with unused Protscore ≥1.68 and FDR<1% were identified, in which over 1,200 proteins were significantly modulated by hypoxia (Supplemental Table S1). Further analysis of the quantitative proteomics dataset indicated that DNA repair, glycolysis, integrin, glycoprotein turnover, and STAT1 pathways were perturbed by hypoxia. Most of them as listed in Supplemental Table S2 were confirmed and validated using WB or LC-MS/MS-MRM methods. Functional studies revealed the roles of the glycolysis, integrin, glycoprotein synthesis and STAT1 pathways in hypoxia-induced cancer metastasis.

Experimental Procedures

Chemicals and Reagents

All reagents were purchased from Sigma Chemical Co. (St. Louis, MO) unless otherwise specified. Antibody against integrin alpha 5 was purchased from Millipore (Billerica, MA). Anti-STAT1 and anti-STAT1 (pS727) were purchased from BD Biosciences Pharmingen (San Jose, CA) and Cell Signaling (Danvers, MA), respectively. Anti-Ku70, Ku80, ITGB1, 1-Deoxynojirimycin Hydrochloride (1-DJ) was purchased from Santa Cruz (Santa Cruz, CA).

Cell culture and hypoxic condition

The A431 epithelial carcinoma cells were purchased from ATCC and maintained in DMEM with 10% FBS. For all experiments, 2 X 10^6 cells were seeded on 10cm dishes in DMEM and incubated under 5% CO_2 at 37°C. Upon reaching 30-40% confluency, the cells were washed with 1X PBS for three times and serum-free media

for three times before incubating in serum-free media. They were subjected to normoxia (Nx: 21% O2/5% CO2) for 72 hr or hypoxia (Hx: <0.1% O2/5% CO2) in a hypoxia chamber for 36 hr or 72 hr. For Reoxygenation (ReOx), the cells were exposed to Hx for 48 h, changed to a fresh medium, and then exposed to Nx condition for an additional 24 h. At least five independent biological replicates were pooled for the analyzed sample in each condition.

Sample Preparation, iTRAQ Labeling, and LC-MS

The cellular proteins were dissolved in 8M urea in 50mM TEAB (pH 8.5) solution with protease inhibitor cocktail (1:50). Protein concentrations were measured using BCA assay. 200µg of proteins from each condition were reduced with 5 mM TCEP at 30°C for 1 hr, alkylated with 10 mM MMTS at room temperature, in the dark for 45 mins. The samples were diluted to 1M urea using 50 mM TEAB and digested by trypsin in a 1:50 mass ratio at 37°C overnight. The solution containing tryptic peptides was adjusted to pH 2-3 with TFA and desalted using Sep-Pak C18 cartridge (Waters). The peptides were dried using speedvac concentrator and, dissolved in 1M TEAB (pH 8.5) and labeled with the isobaric tags (Applied Biosystems, Foster City, CA) according to manufacturer's protocol as followed: the Nx-treated sample was labeled with 114; the samples under Hx for 36 hr or 72 hr were labeled with 115 or 116 respectively; and the ReOx-treated sample was labeled with 117.

The labeled sample was fractionated by a PolySULFOETHYL A column (PolyLC, Columbia, MD; 4.6 ×200 mm, 5µm particle size, 200-Å pore size) using Shimadzu Prominence UFLC system (Kyoto, Japan). Fractionation was performed with a 60-min linear gradient of 0–500 mM KCl (10 mM KH2PO4, pH 3.0, 25% acetonitrile) at

a flow rate of 1 ml/min. A total of 25 fractions were collected and desalted using Sep-Pak C18 cartridges (Waters). Each fraction was dried and reconstituted in 30µl 3% ACN and 0.1% formic acid for LC-MS/MS analysis. All fractions were analyzed using a QSTAR Elite mass spectrophotometer coupled with an on-line Tempo nano-MDLC system. The sample was injected twice. For each injection, 15µl iTRAQ labeled peptide mixture was injected and separated on a home-packed nanobored C18 column with a picofrit nanospray tip (75µm inner diameter×15 cm, 5µm particles) (New Objectives, Woburn, MA). The detailed parameters were set as previous described (3).

Database Searching and Criteria

Protein identification and quantification were performed using ProteinPilot^{TM} software 2.0.1 with Revision number 67476 (Applied Biosystems) by searching the combined raw data from the two runs of labeled sample against the concatenated "target" (Uniprot human database, downloaded on 12 March 2010, including 95624 sequences and 36307192 residues) and "decoy" (the reverse amino acid sequence for false discovery rate (FDR) estimation) databases. The Paragon and Pro Group algorithms in the ProteinPilot software were used for peptide identification and isoform-specific quantification. User-defined parameters were as follows: (i) sample type, iTRAQ 4plex (peptide-labeled); (ii) cysteine alkylation, MMTS; (iii) digestion, trypsin; (iv) instrument, QStar Elite ESI; (v) special factors, none; (vi) species, none; (vii) specify processing, quantitative; (viii) ID focus, biological modifications; and (ix) search effort, thorough ID. Two missed cleavage sites are permitted and non-specific cleavage sites are prohibited. The Mass tolerance of precursor ions and fragment ions is both 0.2 Dalton.

To minimize false positive results, a strict cutoff for protein identification was applied with FDR<1% as listed in Supplemental Table S1. The resulting data set was autobias-corrected to get rid of any variations imparted due to unequal mixing during combining different labeled samples. For iTRAQ quantitation, the peptide for quantification was automatically selected by the Pro Group algorithm (at least one peptide with 99% confidence) to calculate the reporter peak area, error factor (EF), and p value. The proteins for further analysis were filtered with p value <0.05, and 1.2-fold changes (>1.20 or <0.83) relative to the normoxic control unless the proteins were known to be of interest from our functional assay. The list of proteins used is shown in Supplemental Table S2.

Semi-quantitative RT-PCR and Western blotting

Total cellular mRNAs were isolated using TRIzol reagent (Invitrogen, Carlsbad, CA) according to the manufacturer's instructions. cDNA was reversely transcribed from 2 jig total RNA in a final volume of 20 jil using RTase (Promega, Madison, WI, USA). Primer sequences were listed in Supplemental Table S3. PCR was performed with KAPA Fast Taq polymerase in a DNA thermal cycler (PTC-200, Bio-Rad, Hercules, CA) according to a standard protocol as follows: 1 cycle of 95°C for 1 min; 28 cycles of 95°C for 10 s, annealing at 57°C for 10 s, 72°C for 1 s, a final extension at 72°C for 30 s and holding at 4°C. The amount of cDNA used for each PCR reaction was 20 ng in a 25 jil reaction volume. The PCR products (5 jil) were analyzed by electrophoresis through 2% agarose gels and visualized with ethidium bromide staining.

Prior to Western blot analysis, protein concentration of cell lysates dissolved in 1% SDS in 40mM Tris-HCl (pH 8.0) was quantified using BCA assay, equal protein amount from each sample were separated on 12% SDS-PAGE. For native gel, the solution of 1% Triton X-100 in 20mM Tris-HCl (pH 7.4), 150mM NaCl with complete protein inhibitor cocktail (1:50) was used in the extraction of protein complexes. Proteins were then transferred to nitrocellulose membrane and immunoblotted using antibodies against STAT1, p-STAT1, Ku70, Ku80, ITGA5 and ITGB1 respectively. The probe proteins were detected with Invitrogen ECL system according to the manufacturer's instructions.

Dynamic MRM quantification

The same amount of proteins from both normoxic and hypoxic A431 cells were loaded and separated on 12% SDS-PAGE. Based on the proteins molecular weight, each lane was manually excised into six fractions and in-gel digested with trypsin. The peptides were loaded onto 6490 Triple Quadrupole LC-MS/MS system coupled with Infinity 1260 liquid phase separation system (Agilent Technologies Inc, Singapore). The information of all peptides and their transitions of target proteins were obtained from Peptide Atlas (www.peptideatlas.org) database and showed in Supplemental Table S4. All samples were subjected to conventional MRM analysis for confirmation of retention times of peptides. Then dynamic MRM was used to quantify the protein changes.

The mobile phase consisted of solvent A, 0.1% aqueous formic acid and solvent B, acetonitrile with 0.1% formic acid. Peptides were separated by Agilent chip (Large capacity chip II) packed with Zorbax 300SB C18 resin (5μm, separation: 150mm × 75 μm; enrichment: 9mm, 160nL). Injections were 2 μl of a sample solution and were

followed by a 10 min wash period with 100% A, then by elution with a gradient of 0–10% solvent B in 3 min, 10–35% solvent B in 47min, 35-80% in 2min, 80-82% solvent B in 3min and followed by 3% solvent B in 5min.

LC-MS/MS-MRM analyses of the peptide were done with an electrospray voltage of 1700 V, capillary temperature 185°C and skimmer offset −S V. Both Q1 and Q3 were set at unit resolution (FWHM 0.7 Da) and collision gas (N2) pressure in Q2 was held at 1.5 mTorr. Scan width was 0.004 *m/z* and scan time was 20 ms for the peptide. Collision energy for each peptide was calculated based on the equation: CE = (((m/z)/100.0)*3.6 - 4.0), in which the *m/z* is the mass to charge ratio of the precursor ion. Peak areas for each peptide were extracted and integrated using Agilent Qualitative Analysis B.04.00 software.

Construction and transfection of STAT1a expression vectors

The full length of STAT1a was obtained from A431 cDNA library prepared as described above using PCR. The primer information is listed in Supplemental Table S3. The gene with Not I and BamH I enzyme sites were inserted into the expression vector of p3xFLAG-CMV-10 and positive clones were confirmed by plasmid digestion with Not I and BamH I and DNA sequencing. For stable transfection, A431 cells were transfected using 20 µl of lipofectamin 2000 (Invitrogen) and 4 µg of p3xFLAG-STAT1a vector or control p3xFLAG vector according to manufacturer's instructions. Cells were then selected with standard medium with 1mg/ml G418. 2-3 weeks later, the monoclones were picked up and further cultured in medium with 0.5mg/ml G418. The positive clones were confirmed by WB using anti-Flag, STAT1 and phospho-STAT1 antibodies.

Cell proliferation and cell adhesion assay

24-well plates were coated with 5 μg/ml fibronectin in PBS. Uncoated wells were incubated with 0.5 % BSA in DMEM to serve as negative control. Cells were trypsinized and seeded into coated 24-well dish at a density of 2.5 X 10^5 live cells. After incubation for 20 mins to an hour at 37°C, the detached cells were removed by serum-free medium and attached cells were fixed with 95% ethanol for 10 mins and stained with 0.5% crystal violet for 25 mins. The plate was reimmersed in deionised water to remove excess dye and then allowed to air-dry for 5 to 10 mins. The adherent cells were photoed by optical microscopy under 100 x magnification and a total of 200 μl of 0.5% Triton X-100 was added to each well to solubilize the cells overnight at room temperature. The absorbance was measured at OD595 using a microplate reader (Tecan Magellan^{TM}, Männedorf, Switzerland). Cell proliferation was assessed by the ability to exclude 5 mg/ml MTT in PBS for 2 h. MTT uptake was quantified at A_{540nm}, $^{reference}A_{630nm}$ after solubulization in DMSO.

Cell staining

To visualize ITGA5 distribution in cells, immunofluorescent staining with anti-integrin a5 antibody was performed. A431 cells were seeded into 20 X 20-mM coverslips, treated for the indicated conditions, fixed by 4% paraformaldehyde, and then permeabilized with 0.2% Triton X-100 in PBS for 10 mins. The cells were incubated with 4% BSA in 0.1% Triton X-100 for 20 mins to block nonspecific binding sites before incubation with anti-ITGA5 in 1% Triton X-100 (Millipore; 1:100) for 2 h at 37°C. Subsequently, the cells were washed, and then incubated with Alexa Fluor® 488-conjugated secondary antibody for 1 h at room temperature. After that, cells were washed, mounted, and examined by fluorescence microscope.

Scratch-wound assay

2 X 10^6 cells were seeded in a 6-well plate. A wound was made by scratching the cells in a line with a sterile pipette tip in the middle of the well next day. Then cells were washed twice with 1 X PBS and three times with serum free media before incubating in serum-free media. Photographs were captured by a Nikon Eclipse TE2000-U microscope. After incubation in indicated conditions under hypoxia for specific time points shown in Fig. 2, 4 and 6, photographs were taken again. Hypoxic treatment was the same as above mentioned. For 1-DJ wound-scratch assay, the cells were treated by the drug for 48 h and then undergone scratch assay under hypoxia. After hypoxia, the cells were lysed with 1% SDS solution and used for WB to detect their glycoproteins by HRP-labeled lectin. Since 2-DG and 1-DJ are water soluble, no control solvents are used in the experiments. The migration of cells into the wound was recorded and the wound closure was determined.

Metabolite analysis

For A431 cell metabolite extraction, MeOH/H2O (80:20) solution was used as described in published paper because the solution had been proved to be a more suitable extraction solvent (36). Briefly, after the same amount of A431 cells were treated with or without 2-DG or hypoxia, the growth medium was discarded and cells were rapidly washed three times with cold PBS followed by adding cold MeOH/H2O (80:20), which caused protein precipitation and hence cell disruption. Wells were then lightly scraped with a rubber tipped cell scraper. The dishes were washed two times with MeOH/ H2O solution and the wash and the extract solution were combined for centrifuging at 4 °C and 5,725×g for 5 min. The supernatant was collected for dry. All

steps were performed on ice. The metabolites were solved in 0.1% FA for ESI-Q-TOF analysis. Metabolite levels were normalized to protein content in the pellet after metabolite extraction, which was determined by the 2D-Quant Kit (GE Healthcare, Munich, Germany)(36, 37).

The same amount of metabolites normalized with protein level was directly injected to mass spectrometer with 10μL/min flow. Negative-ion mode electrospray mass spectra were obtained using an Accurate-Mass Q-TOF LC/MS 6530 (Agilent Technologies). Spray voltage was −1.0kV and the capillary temperature was set to 185 °C. Spectra were collected in full scan mode in a scan range of 50–400 m/z. The precursors with very close m/z with metabolites in glycolysis pathway were chosen for MS/MS identification. MS/MS spectra were obtained using isolation width 4 m/z, and scan rate 1 spectra/s, with collision energy -9.The m/z and intensity of MS/MS spectra was input to Massbank database for metabolite identification (http://www.massbank.jp/MetaboIdentif.html).

Statistical analysis

The measurements were expressed as mean ± SD. The paired t-test was used for statistical analysis between two groups. Significant level was set at $p < 0.05$.

Results and Discussion

Proteomic analysis of Normoxic, Hypoxic and Reoxygenated A431 cell lysate

The iTRAQ reagent labeled peptides were quantitatively profiled by LC-MS/MS using QStar Elite MS. The expression level changes of proteins were indicated by the ratios of labeling tag (N72:114; H36:115; H72:116; H48+R24:117). Raw data were analyzed using ProteinPilot 2.0.1 software with autobias correction against the

UniProt human database. A total of 4,316 proteins were identified with unused score ≥ 1.68 and FDR <1% (Supplemental table S1). iTRAQ reporter ratios of 1.2 and 0.83 were set as the cut-off of protein changes. Totally 1,253 proteins were found responsive to hypoxia. These proteins have at least one ratio with p-value<0.05, including 522 up-regulated and 743 down-regulated (Table 1 and Supplemental table S1). All of the data including wiff raw data from QStar, searched group file from ProteinPilot 2.0.1 and the search results of PeptideSummary and ProteinSummary can be downloaded from ProteomeCommons.org Tranche Network using the following hash
(Q85ii60OE5SelJDghF4vp2Gjv/dJndWgdMF8yZlmbqXeYgOCLVMBsRz840rGKE oyovesJyYL3rmak5baMgCRO5UBWKoAAAAAAAAZ9Q==; for wiff raw data set A;
1G135KGPNp+aETVXL7j5VSBfJDYGNshh6mDkHTpC7eXYzFWn5gq1xfx69LP/q HPaOpnyDd37dlB+auqnmWCSwFSeczQAAAAAAAAZ9Q==; for wiff raw data set B;
LjkJyHVkOJU59YzP26G6Q5ozCw6Iy1XQQfNNGoDZaL8wrbE0eav3TNatlUL2z3d hsqz17RXpx7v2pgxYiIHBe9MV0I8AAAAAAAAB0Q==; for searched group file;
MAFBxhUOXAz2nHHgcMZszGUCRewTyg0hoHJ/a5CWtGTr9/ZxYOeYc5yJgrRW 9W8jhJawUjdA9bNfdN0HUiwsXBnzYC8AAAAAAAACGg==; for PeptideSummary;
StQPOjfbpRPzCc3AP4SCSL6hzckua/anydKvaG0TSvim5DdFDFpXucq+n6MMpvdn 7CFycO1R6xhLp7lOOx5OTpHSrNcAAAAAAAACDQ== for ProteinSummary).

The high quality iTRAQ quantitative datasets provided invaluable biological insight on hypoxia induced tumor progression. To gain the global insights of these proteins, Ingenuity Pathway Analysis (IPA, Ingenuity® Systems, www.ingenuity.com) platform was used to analyze the data to reveal the molecular and cellular functions and canonical pathways induced by hypoxia stress. All the proteins listed in Supplemental Table S1 were used for IPA. The up-regulated and down-regulated proteins were analyzed separately, and thus these proteins were mapped to different function, pathway and toxic lists. The summary of IPA was listed in Supplemental Figure S1 including top five function, pathway and tox lists that up-regulated and down-regulated proteins involved. The top changes in function and pathway were those regulating basic cell survival, for example, protein synthesis and degradation, post-transcriptional or translational modification, protein folding and trafficking and energy and material metabolism. The top toxic lists were mainly involved in

mitochondrial dysfunction, oxidative stress and HIF signaling, which indicated the impact of hypoxia on cellular functions. The proteins involved in HIF signaling pathways were shown down-regulated after hypoxia because the top one pathway down-regulated under hypoxia is ubiquitination degradation pathway and the increased expression of HIF-1a was primarily due to increased protein stabilization via decreased ubiquitination degradation. The pathways with dominant difference in comparison analysis of down-regulated and up-regulated proteins were chosen for further studies (Supplemental Figure S2 and Supplemental Table S2). The proteins mapped to STAT1 (down-regulated pathway) and N-glycosylation degradation (up-regulated pathway) were illuminated in Supplemental Figure S3.

Hypoxia activated A431 NHEJ pathway in DNA repair

Ionizing radiation causes cell death primarily by DNA double strand breaks (DSBs). The two main pathways involved in the repair of DSBs are homologous recombination (HR) and nonhomologous end-joining (NHEJ) pathways. Of the two, NHEJ pathway generally considered to be an error prone pathway is the dominant repair pathway in radiation-induced DNA damage (38). Our iTRAQ data showed that hypoxia substantially increased A431 proteins involved in DNA repair, especially those responsible for DSB repair in the NHEJ pathway (Fig. 1A). When DNA DSBs occurred, Ku70 and Ku80 bind rapidly with the DNA ends, promoting the inward sliding of Ku70 and Ku80 along the length of DNA, at the same time recruiting PRKDC to assemble a DNA-PK heterotrimer(39). Formation of this complex may also be promoted through interactions with heterodimeric ILF2 and ILF3(40). Our proteomic data showed that all of these proteins (Ku70, Ku80, PRKDC, ILF2 and ILF3) were up-regulated under hypoxic conditions (Fig.1A). Subsequent phosphorylation of DNA-PKcs destabilizes and causes the complex to dissociate, allowing the recruitment of several end-processing enzymes including ligase IV, NHEJ1 and Mre11 /Rad50/ Nbs1 proteins of the MRN complex to DNA. Two of them, NHEJ1 and Rad50 were shown to be up-regulated in our data (39). In addition, the proteins that favour DSBs repair were also up-regulated under hypoxia. These include MDC1, SFPQ, NONO, SSRP1, SUPT16H, INTS3, APTX and PRPF19. MDC1 and SFPQ-NONO heterodimer have been shown to facilitate the DNA repair in NHEJ pathway (41, 42). SSRP1-SUPT16H dimers, INTS3, APTX and PRPF19 also have been proven to stabilize DSB repair (43-46). The expression level and heterodimer changes of Ku70 and Ku80 were validated by LC-MS/MS-MRM and Western blot (Fig. 1B and 1C). In dynamic MRM quantification results, TBB6 and ACTN1,

housekeeping proteins, and ATP5B were used as internal controls as their expression levels assessed by iTRAQ were not modulated by hypoxia. The peptides of TBB6, ACTN1 and ATP5B with several strong transitions as shown in Supplemental Table S4 were quantified in dynamic MRM with ratios of 0.92 ± 0.07, 0.90±0.07 and 0.96 ± 0.09 respectively. The copy numbers of the two peptides from Ku70 with seven transitions showed significant increase to 2.86 ± 0.78 folds under hypoxia stress. The intensity of four peptides of Ku80 under hypoxic condition was also higher (2.05±0.69) than that of peptides under normoxic condition (Fig. 1C and Supplemental Table S4). Their change ratios are much higher than those of Ku70 and Ku80 in iTRAQ quantification results (with ratios 1.1-1.2). In addition, the increase of another key component of DNA-PK heterotrimer, PRKDC1, and other components of the NHEJ pathway (ILF2, NONO, SP16H, PRP19 SFPQ, SSRP1 and APTX) during hypoxia was also verified by MRM method (Fig.1C and Supplemental Table S4). The slight changes of Ku70 and Ku80 observed from iTRAQ data were further validated by SDS-PAGE WB that confirmed increased expression (with ratios less than 2.03) of both proteins as shown in Fig.1B (the upper two panels). As formation of Ku70/Ku80 heterodimer are prerequisites for functional activity, protein extracts from the tumor cells were separated on native gels and analyzed for the presence of Ku70/Ku80 heterodimer using antibodies against either Ku70 or Ku80. Both antibodies detected the same single band on the native gel which indicated the Ku70/Ku80 dimer position (the lowest panel in Fig. 1B). The WB results clearly showed obvious increase of heterodimer under hypoxia. To further confirm the result and avoid the interference from cellular proteins, we isolated chromatin of A431 under normoxia and hypoxia using sucrose gradient, and quantified the chromatin binding proteins using iTRAQ analysis. Result showed that the key proteins in NHEJ pathway, such as Ku70, Ku80, PRKDC1, associated with chromatin increased under hypoxic condition (unpublished data). In 2008, for the first time, a decrease in Ku70 and Ku80 was found to be present in more hypoxic cervical carcinoma tissue by immunohistochemistry; however, the results were not further validated (38). Our quantitative proteomic data for the first time showed that hypoxia increased most components of the NHEJ pathways in A431. As these components have been implicated in mediating ionizing radiation resistance, our data also provided a possible molecular mechanism for hypoxia-induced radiation resistance.

Hypoxia induced cell migration through metabolic switch from TCA cycle to glycolytic pathway

It has been well known that tumor cells exhibit increased rates of glucose uptake and glycolysis (47). Increased glycolysis in tumor cells is regarded as an effect of intratumoral hypoxia. Under hypoxic conditions, cells switch their form of glucose metabolism from the oxygen-dependent tricarboxylic acid (TCA) cycle to glycolysis, an oxygen-independent metabolic pathway. HIF-1 has been shown to activate transcription of genes that encode glucose transporters GLUT1, GLUT3 and all glycolytic enzymes (2, 48). In our iTRAQ data, the enzymes that catalyze the four steps in glycolysis pathway, hexokinase(HK), glucose 6-phosphate isomerase(G6PI), fructose-bisphosphate aldolase (ALDOA and FBPA) and biphosphoglycerate kinase (PGK) were all found to be up-regulated after hypoxia. The enzyme that regulates pyruvic acid efflux, lactate dehygrogenase A (LDHA), was also significantly up-regulated under hypoxia (Fig. 2A). Surprisingly, enzymes that are involved in the TCA cycle such as pyruvate dehydrogenase (PDHB), citrate synthase (CS), isocitrate degydrogenase (IDH2), a-ketoglutarate dehydrogenase (DHTKD1), fumarase (FH), malate dehydrogenase(MDH1) and pyruvate carboxylase (PC) were down-regulated under hypoxia (Fig. 2B). LC-MS/MS-MRM analysis results showed that the enzymes of HK, ALDOA, PGK1 and GPI in glycolysis pathway were also found obviously up-regulated as detected by iTRAQ analysis under hypoxia (Supplemental Table S4). Increased glycolysis has been associated with tumor invasiveness, metastasis and/or resistance to therapies (49). Recently, Cai *et al.* highlighted this relationship between glycolysis and metastasis in cancer cells by knocking down LDHA or overexpressing PDHB to force pyruvate into TCA cycle rather than the glycolysis process. This inhibited cellular growth and migration of gastric cancer cells (50). Our iTRAQ and MRM quantification data both indicated the increase of LDHA and the decrease of PDHB after hypoxia treatment (Fig. 2A, 2B and Supplemental Table S4). In support of this link between glycolysis and metastasis, Izumi *et al*. also reported that knockdown of monocarboxylate transporters (MCT1 and MCT4) led to reduced invasiveness of human lung cancer cells (51). Since MCT1 and MCT4 transport monocarboxylate such as lactate across membranes and are important in maintaining continuous glycolysis, their knockdown would result in reduced glycolysis. In view of this, the up-regulation of monocarboxylate transporter, SLC16A1 (MCT1) under hypoxic conditions as observed in our study (Fig. 2A) would enhance continuous glycolysis. In addition to MCT1, glucose transporter SLC2A1 (GLUT1) was also found up-regulated in iTRAQ and MRM quantification results (Fig. 2A and Supplemental Table S4). Since down-

regulation of GLUT1 inhibits cellular glucose uptake, growth, and invasiveness of MG63 cells (52), its up-regulation under hypoxia would enhance cellular glucose uptake, growth, and invasiveness. Based on these data, we hypothesized that cells increased proteins that will enhance glycolysis and promote metastasis during hypoxia.

2-Deoxy-D-glucose (2-DG) is one of the best characterized glycolysis inhibitor in animal model studies and human clinical trials (53, 54). In scratch-wound assay, 2-DG at a higher concentration was used to treat A431 cells and suppress the glycolysis pathway. The cell migration was found to be significantly inhibited when compared with that of the control cells under hypoxia and this reduced migration appeared to show positive correlation to the concentration of 2-DG (Fig. 2C). After exposure of A431 cells to 10 mM or 15 mM 2-DG for 20 h, cell migration into the wounded region of A431 cells was reported to be 65.9 ± 9.4% and 36.3 ± 5.9% as compared to control cells, respectively (Fig. 2D). The inhibition of 2-DG to cell glycolysis pathway was confirmed by metabolite analysis using LC-ESI-Q-TOF. The TIC of control metabolite sample had a slight higher peak than that of 2-DG treated cells, which indicated the loading amount of control and 2-DG treated samples was similar and the normalization with protein content is relatively accurate (Supplemental Fig. S4A). However, the EIC peaks of one intermediate of glycolysis pathway, Fructose 1,6-biphosphate (FBP, m/z:339.12), extracted from TICs had obvious difference. The area of EIC peak from control sample is about 12 folds of that of 2-DG treated sample (Supplemental Fig. S4B). FBP level in normoxic and hypoxic A431 was also detected using the same method. This glycolysis metabolite in hypoxia sample is up-regulated compared with normoxia sample even with a lower TIC in hypoxia sample during MS analysis (Supplemental Fig. S4C and D). Supplemental Fig. S4E is referred to the MS/MS fragments of the precursor 339.12. The m/z and intensity of these MS/MS fragments was input to Massbank database for metabolite identification (http://www.massbank.jp/MetaboIdentif.html). Only the Fructose 1,6-biphosphate of metabolite was matched. These results clearly showed that 2-DG inhibited, but hypoxia activated glycolysis pathway. Though 2-DG also resulted in the inhibition of glycan biosynthesis of glycoproteins, thus reducing the glycoproteins in cells and cell adhesion, treatment with glycan biosynthesis inhibitor (1-Deoxynojirimycin Hydrochloride, a glucose analog that inhibits α-glucosidase I and II activity) during the scratch assay for 20 h had no effects in cell migration (data not shown). These results indicate that the activation of glycolysis under hypoxic conditions is associated with enhanced A431 cell migration ability.

Hypoxia induced overexpression of intergrins and their ligands: implication for increased metastasis

Integrins, a major family of adhesion proteins, are involved in numerous physiological and pathological processes, including inflammation, wound repair, proliferation, differentiation and apoptosis (55, 56). In particular, they play a crucial role in metastasis. It is well established that fibronectin-integrin complexes played direct and indirect roles in signaling pathways that are involved in adhesion, migration, apoptosis, and growth (57). Expression of fibronectins and integrins are up-regulated in migratory cells in promoting of cell migration (58). Each integrin is composed of 2 subunits, namely α and β subunits. 18α and 8β integrin subunits assemble into 24 distinct receptors in mammals (59). Our iTRAQ data revealed the up-regulation of several integrin subunits under hypoxic conditions. The changes were partially reversed by reoxygenation (Fig. 3A). ITGα5β1 is one of the important integrin molecules. The increase expression of ITGA5 and ITGB1 subunits under hypoxia was validated by WB and LC-MS/MS-MRM methods (Fig. 3B and Supplemental Table S4). Both results clearly showed that hypoxia induced the expression of the two subunits. Cell staining results not only showed the up-regulation of ITGA5 but also their recruitment to the plasma membrane under hypoxic conditions. ITGA5 appears to be evenly distributed in the normoxic A431 cells, whereas it has been observed to reside in the plasma membrane of both hypoxic and reoxygenated cells (Fig. 3C). LC-MS/MS-MRM experiment also confirmed up-regulation of other integrin molecules (ITGA3, ITGA6 and ITGB4) in A431 cells under hypoxia, indicating hypoxia may increase cell adhesion (Supplemental Table S4). We thus examined the adhesion ability of A431 cells on matrix-coated dishes after pre-exposure to hypoxia. The adhesion assay proved that hypoxia induces increased adhesiveness of A431 cells pre-exposed to hypoxia within 20 mins of seeding onto the fibronectin-coated dishes (Fig. 3D). The adhesion of the hypoxic and reoxygenated cells to fibronectin is approximately 134.5 ± 4.2% and 121.4 ±5.5% of that of normoxic cells, respectively (Fig. 3E). This increase in cell adhesion was consistent with the increase of several integrin molecules and ITGA5 recruitment to the plasma membrane. It has been reported that up-regulation of ITGA5 and fibronectin mediated by hypoxia, is responsible for the increased invasiveness of cancer cells (60). In hypoxia, the loss of E-cadherin leads to the up-regulation of ITGA5, resulting in the increased migration of extravillous trophoblast cells during early implantation (29). Integrins have a wide binding range to matrix proteins, which include laminin, fibronectin, trombospondin, vitronectin and the various types of collagen (61). The cell

adhesion ligands including several lamimin and collagen subunits were also found to be up-regulated under hypoxia (Fig. 3F). Hypoxia induced factor 1 (HIF-1a) directly regulates the promoter activity of laminin a3 chain of laminin-332 (formerly laminin-5) and contributes to the migration of keratinocyte by increasing the expression of laminin-332 (62).

Hypoxia induced higher turnover rates of glycoproteins

Glycoproteins play important roles in a wide range of biological events, including bacterial and viral infections, the metastasis of tumor cells, immune responses, and fertilization and differentiation (63). There are two major types of glycoproteins in mammalian cells, N-linked and O-linked glycoproteins. The synthesis and breakdown of N-linked glycoproteins have been studied intensively. The biosynthesis of the various types of N-linked oligosaccharide structures involves two series of reactions: 1) the formation of the lipid-linked saccharide precursor, Glc3Man9(G1cNAc)2-pyrophosphoryl-dolichol, by the stepwise addition of G1cNAc, mannose and glucose to dolichyl-P, and 2) the removal of glucose and mannose by membrane-bound glycosidases and the addition of G1cNAc, galactose, sialic acid, and fucose by Golgi localized glycosyltransferases to produce different complex oligosaccharide structures (64). Glycosidases are key enzymes involved in the biosynthesis of N-linked glycoproteins as they hold critical role in the formation of hybrid and complex types of N-linked oligosaccharides (65). Glycoproteins are degraded in lysosomes. Once inside the lysosome, glycoproteins are broken down by a combination of proteases and glycosidases. We found that, for the first time, the turnover of glycoproteins is regulated and promoted by increase of enzymes involved in biosynthesis and breakdown of glycoproteins under hypoxia (Fig. 4A and 4B).

The iTRAQ data showed that the enzymes (ALG1, ALG2 and DPM1), involved in the formation of lipid-linked saccharide precursor by transferring mannose in N-linked oligosaccharide formation step 1, were up-regulated under hypoxia. The glycosidase (MA1B1and MAN2A1) responsible for the removal of mannose, MOGS for glucose removal and the glycosyltransferases (Oligosaccharyltransferase complex, OST) in the step 2 of N-linked glycan synthesis were also found to be up-regulated. OST exists in different forms, namely RPN1, RPN2, OST48, DAD1, OSTC, KRTCAP2 and either STT3A or STT3B, which catalyzes the transfer of a high mannose oligosaccharide from a lipid-linked oligosaccharide donor to an asparagine residue within an Asn-X-

Ser/Thr consensus motif. RPN1, RPN2, OST48, DAD1, OSTC, STT3A and STT3B were found in higher expression in hypoxia. In addition, the enzymes for O-linked glycan formation (GALNT2, C1GALT1 and GLT25D1) were also up-regulated in hypoxia. The enzymes for glycoprotein catabolism in lysosomes including proteases and glycosidases were induced by hypoxia too. The cathepsins (CTSA/B/C/D/H/Z) for polypeptide degradation and glycosidases (HEXA, HEXB, MAN2B1, GLB1 and FUCA1) for cleavage of N-acetyl hexosamines, α-mannose, β-galactose, and α-fucose, respectively, were found to undergo similar change pattern during hypoxia and reoxgenation (Fig. 4B).

We speculated that the quantitative changes in glycosylation enzymes during hypoxia would affect glycoproteome and that this change would be associated with cell metastasis because of the important roles of glycoproteins in tumor cell metastasis. 1-Deoxynojirimycin (1-DJ), an analogue of glucose that contains an NH group substituting for the oxygen atom of the pyranose ring, inhibits Golgi alpha-glucosidase and thus inhibits glycoprotein synthesis. This drug was used to treat A431 and perturb the glycoprotein-turnover under hypoxia. Short term drug treatment (20h) exhibited no prominent effect upon cell migration in scratch assay and this result also was supported by the reported data (66). However, once A431 cells were treated with 100μM 1-DJ for 48h, the cells displayed slower migration than non-treated cells under hypoxia (Fig. 4C). The migration into wound of A431 cells treated by 100 μM 1-DJ is only 72.3% ± 12.6% of that of control cells (Fig. 4E). The lectin binding result showed that the synthesis of glycoproteins in A431 was inhibited after 1-DJ and hypoxia treatment (Fig. 4D). These data indicate that hypoxia contributes to A431 enhanced migration by increasing glycoprotein synthesis and modulating glycoprotein turnover.

Hypoxia promoted A431 migration by suppression of STAT1 pathway

Thus far, studies determining the influence of hypoxia on protein expressions have been restricted to proteins with enhanced expressions. Only a few studies have been done on proteins whose expression is down-regulated by hypoxia (35). STAT1, the first described member of the STAT transcription factor family, is the master transcription factor for IFN-related intracellular signaling (67). STAT1 has two isoforms, STAT1a and STAT13. The 3 isoform lacks the 38 residues encompassing the transcription activation domain at C-terminal and is transcriptionally inactive (68).

STAT1a is phosphorylated by JAK1/2 kinases at the Tyr701 position and then translocates to the nucleus where it binds to GAS (IFNc-activated sequence) promoter elements, thereby activating several hundred genes (69). Phosphorylation of STAT1a at S727 is essential for activating transcription of target genes and interaction with proteins, such as BRCA1 and MCM-5, potentiating STAT1-mediated transcription (70-73).

STAT1 and its downstream proteins (MX1, IFIT1, IFIT3, ISG15 and PSMB8) were significantly down-regulated under hypoxia as reflected in our proteomic data (Fig. 5A), the suppression of STAT1, PSMB8 and IFIT1 was confirmed by MRM quantification (Supplemental Table S4). The significant decline of total STAT1 was further confirmed by WB experiment. The active isoform of STAT1 was also shown to be highly suppressed by hypoxia because the anti-pSTAT1(S727) only recognizes STAT1a isoform with transcriptional activity (Fig. 5B). The mRNA level changes of STAT1a detected by its specific primers and its downstream genes were validated by RT-PCR. Fig. 5C clearly indicated their suppressed transcription as a result of STAT1a down-regulation after hypoxia. STAT1 dramatically increases the transcription of IRF-1 through the interaction with NF-κB or in response to IFN (74, 75). IRF-1 transcription was suppressed in response to decreased STAT1 in RT-PCR; however, as a specific inhibitor of STAT1, PIAS1 showed a reverse finding with STAT1 (76). The alteration of STAT1 expression level due to hypoxia at present remains controversial. Several studies have reported that hypoxia led to activation of STAT1, especially in cardiomyocytes (77-80). Paradoxically, Ivanov *et al.* reported that STAT1 and its downstream genes can be repressed by a pVHL/HIF-1 target DEC1/STRA13 in carcinoma cells under hypoxia (81).

In order to get more evidence of STAT1 functions under hypoxia, two A431 stable cell lines with STAT1a overexpression were screened for further studies. The human cDNA of STAT1a was inserted into p3xFLAG-CMV-10 expression vector and transfected into A431. G418 was used to screen the cell line stably overexpressing STAT1a. The positive clones were confirmed by WB using anti-FLAG and STAT1 antibodies. When compared with the control cell line transfected with empty p3xFLAG-CMV-10, FLAG-STAT1 was only detected in the STAT1a stable cell lines (A431-p3XFLAG-ST1a-1 and 2). The stable cell lines also showed higher expression level of STAT1 and phosphorylated STAT1a, in which A431-p3XFLAG-ST1a-2 has a higher expression of STAT1a than A431-p3XFLAG-ST1a-1 (Fig. 5D). RT-PCR

results showed up-regulation of STAT1 downstream genes (Fig. 5E). In summary, the results highly suggest that the stable cell lines with more active STAT1a expressed could be used for functional studies.

MTT was used to evaluate the proliferation/survival of the STAT1a stable cell lines under nomorxia and hypoxia. Under nomorxia, there was no significant difference in the proliferation between control and STAT1a overexpression cell lines. But under hypoxia, STAT1a cell survival suffers a greater decline as compared to control cells and A431-p3XFLAG-ST1a-2 with the highest STAT1a level has a maximum decline (Fig. 6A). These results indicated that A431 cells increased their survivability through the down-regulation of STAT1 under hypoxia. STAT1 has been implicated in the inhibition of cell proliferation in several cell systems by inducing the expression of cyclin kinase inhibitors and caspases in response to extracellular stimuli (82-86). It is also reported that STAT1 can repress HIF-1-mediated transcription after hypoxia (87).

Since hypoxia induces cancer cell migration and causes functional suppression of STAT1, we went on further to examine the effects of STAT1 overexpression on the migration ability of cancer cells under hypoxia. In the scratch-wound assay, statistical results showed that STAT1a overexpression resulted in the repression of A431 cell migration. The migration of A431-p3XFLAG-ST1a-1 and 2 cells is only 82.9 ± 4.3% and 62.0 ± 5.4% of that of A431-p3XFLAG control cells (Fig. 6B and 6C). The migration of A431-p3XFLAG-ST1a-2 is significantly lower than that of A431-p3XFLAG-ST1a-1 due to its higher expression of STAT1a, which shows negative regulation of STAT1 in tumor metastasis. STAT1 has been reported to suppress the metastasis of STAT1-reconstituted RAD-105 cells through the reduction of MMP-2 and MMP-9 *in vivo* and arrest monocyte migration by modulating RAC/CDC42 pathways (88, 89). Our studies further revealed that STAT1a might suppress A431 cell migration by promoting cell adhesion. In adhesion assay, the adhesion ability of A431-p3XFLAG-ST1a-1 and 2 to fibronectin was much higher than that in control cell. After 30 mins incubation, the adhesion cell amount of A431-p3XFLAG-ST1a-1 and 2 is about 2.03 ± 0.03 and 2.28 ± 0.12 folds of that of A431-p3XFLAG (Fig. 6D and 6E). Cell adhesion receptors play important roles in promoting migration; however, the establishment of strong adhesion inhibits migration, which is fastest at optimum adhesion strength strong enough to support traction yet weak enough to allow rapid detachment of the rear of the cell (58). The above results provide evidences that hypoxia induces cell migration by down-regulation of STAT1 because overexpression STAT1 can inhibit migration by enhancing cell adhesion.

Conclusion

In this study, based on iTRAQ quantification data, the pathways associated with tumor radioresistance and migration induced by hypoxia were identified and validated. For the first time, most key molecules in NHEJ pathway, which occurs more often than homologous repair in radiated cells, were found up-regulated under hypoxia and confirmed by LC-MS/MS-MRM and WB. Thus, the proteins in this pathway may provide new targets for molecular therapy in support to radiotherapy (90). In addition, we report hypoxia perturbed the expression of enzymes in glycoprotein synthesis and degradation to modulate glycoprotein turnover. Inhibiting glycoprotein synthesis by small molecule inhibitors under hypoxia led to decrease in cell migration. Glycosylation undergoes a dramatic transformation during cancer malignancy. But only a few structural changes have been frequently correlated with tumor progression by altering specific enzymes for further modification of glycans in Golgi (91). It is an intriguing question to find whether improvement of glycoprotein turnover contributes to the glycosylation transformation during tumor malignancy. STAT1 and its downstream genes were significantly suppressed by hypoxia. The repression is believed to promote cell migration because overexpression of STAT1a can inhibit migration by enhancing cell adhesion. STAT1 has been reported to be inhibited by HIF-1 (81). How about the NHEJ and glycoprotein turnover pathway proteins? It is our future work to knockdown HIF-1 and to investigate its impact on the two pathways under hypoxia. Our findings add in new dimension to our present understanding to tumor hypoxia and provide potential new therapy targets for tumor therapy.

Acknowledgements:

This work is supported by grants from Nanyang Technological University (RG 157/06, RG 61/06 and RG 51/10).

References

1. Brown, J. M., and Giaccia, A. J. (1998) The unique physiology of solid tumors: opportunities (and problems) for cancer therapy. *Cancer Res* 58, 1408-1416.
2. Harris, A. L. (2002) Hypoxia--a key regulatory factor in tumour growth. *Nat Rev Cancer* 2, 38-47.
3. Park, J. E., Tan, H. S., Datta, A., Lai, R. C., Zhang, H., Meng, W., Lim, S. K., and Sze, S. K. (2010) Hypoxic tumor cell modulates its microenvironment to enhance angiogenic and metastatic potential by secretion of proteins and exosomes. *Mol Cell Proteomics* 9, 1085-1099.
4. Wilson, W. R., and Hay, M. P. (2011) Targeting hypoxia in cancer therapy. *Nat Rev Cancer* 11, 393-410.
5. Gray, L. H., Conger, A. D., Ebert, M., Hornsey, S., and Scott, O. C. (1953) The concentration of oxygen dissolved in tissues at the time of irradiation as a factor in radiotherapy. *Br J Radiol* 26, 638-648.
6. Moulder, J. E., and Rockwell, S. (1987) Tumor hypoxia: its impact on cancer therapy. *Cancer Metastasis Rev* 5, 313-341.
7. Le Q.T., Giaccia A.J., and Brown J.M. (2005) The role of tumor hypoxia in head and neck cancer radiotherapy. *Current Clinical Oncology*, 145-163.
8. Liu, J., Zhang, J., Wang, X., Li, Y., Chen, Y., Li, K., Yao, L., and Guo, G. (2010) HIF-1 and NDRG2 contribute to hypoxia-induced radioresistance of cervical cancer Hela cells. *Exp Cell Res* 316, 1985-1993.
9. Moeller, B. J., and Dewhirst, M. W. (2006) HIF-1 and tumour radiosensitivity. *Br J Cancer* 95, 1-5.
10. Markowska, J., Grabowski, J. P., Tomaszewska, K., Kojs, Z., Pudelek, J., Skrzypczak, M., Sobotkowski, J., Emerich, J., Olejek, A., and Filas, V. (2007) Significance of hypoxia in uterine cervical cancer. Multicentre study. *Eur J Gynaecol Oncol* 28, 386-388.
11. Dellas, K., Bache, M., Pigorsch, S. U., Taubert, H., Kappler, M., Holzapfel, D., Zorn, E., Holzhausen, H. J., and Haensgen, G. (2008) Prognostic impact of HIF-1alpha expression in patients with definitive radiotherapy for cervical cancer. *Strahlenther Onkol* 184, 169-174.
12. Tribius, S., Pidel, A., and Casper, D. (2001) ATM protein expression correlates with radioresistance in primary glioblastoma cells in culture. *Int J Radiat Oncol Biol Phys* 50, 511-523.
13. Munshi, A., Kurland, J. F., Nishikawa, T., Tanaka, T., Hobbs, M. L., Tucker, S. L., Ismail, S., Stevens, C., and Meyn, R. E. (2005) Histone deacetylase inhibitors

radiosensitize human melanoma cells by suppressing DNA repair activity. *Clin Cancer Res* 11, 4912-4922.

14. Meng, A. X., Jalali, F., Cuddihy, A., Chan, N., Bindra, R. S., Glazer, P. M., and Bristow, R. G. (2005) Hypoxia down-regulates DNA double strand break repair gene expression in prostate cancer cells. *Radiother Oncol* 76, 168-176.

15. Bindra, R. S., Schaffer, P. J., Meng, A., Woo, J., Maseide, K., Roth, M. E., Lizardi, P., Hedley, D. W., Bristow, R. G., and Glazer, P. M. (2004) Down-regulation of Rad51 and decreased homologous recombination in hypoxic cancer cells. *Mol Cell Biol* 24, 8504-8518.

16. Bindra, R. S., Schaffer, P. J., Meng, A., Woo, J., Maseide, K., Roth, M. E., Lizardi, P., Hedley, D. W., Bristow, R. G., and Glazer, P. M. (2005) Alterations in DNA repair gene expression under hypoxia: elucidating the mechanisms of hypoxia-induced genetic instability. *Ann N Y Acad Sci* 1059, 184-195.

17. Bindra, R. S., Gibson, S. L., Meng, A., Westermark, U., Jasin, M., Pierce, A. J., Bristow, R. G., Classon, M. K., and Glazer, P. M. (2005) Hypoxia-induced down-regulation of BRCA1 expression by E2Fs. *Cancer Res* 65, 11597-11604.

18. Graeber, T. G., Osmanian, C., Jacks, T., Housman, D. E., Koch, C. J., Lowe, S. W., and Giaccia, A. J. (1996) Hypoxia-mediated selection of cells with diminished apoptotic potential in solid tumours. *Nature* 379, 88-91.

19. Young, S. D., Marshall, R. S., and Hill, R. P. (1988) Hypoxia induces DNA overreplication and enhances metastatic potential of murine tumor cells. *Proc Natl Acad Sci U S A* 85, 9533-9537.

20. Brizel, D. M., Scully, S. P., Harrelson, J. M., Layfield, L. J., Bean, J. M., Prosnitz, L. R., and Dewhirst, M. W. (1996) Tumor oxygenation predicts for the likelihood of distant metastases in human soft tissue sarcoma. *Cancer Res* 56, 941-943.

21. Cairns, R. A., and Hill, R. P. (2004) Acute hypoxia enhances spontaneous lymph node metastasis in an orthotopic murine model of human cervical carcinoma. *Cancer Res* 64, 2054-2061.

22. Fyles, A., Milosevic, M., Hedley, D., Pintilie, M., Levin, W., Manchul, L., and Hill, R. P. (2002) Tumor hypoxia has independent predictor impact only in patients with node-negative cervix cancer. *J Clin Oncol* 20, 680-687.

23. Liotta, L. A., Kleinerman, J., Catanzaro, P., and Rynbrandt, D. (1977) Degradation of basement membrane by murine tumor cells. *J Natl Cancer Inst* 58, 1427-1431.

24. Montagner, M., Enzo, E., Forcato, M., Zanconato, F., Parenti, A., Rampazzo, E., Basso, G., Leo, G., Rosato, A., Bicciato, S., Cordenonsi, M., and Piccolo, S.

(2012) SHARP1 suppresses breast cancer metastasis by promoting degradation of hypoxia-inducible factors. *Nature* 487, 380-384.

25. Sahai, E. (2007) Illuminating the metastatic process. *Nat Rev Cancer* 7, 737-749.

26. Horwitz, A. R., and Parsons, J. T. (1999) Cell migration--movin' on. *Science* 286, 1102-1103.

27. Yoon, S. O., Park, S. J., Yun, C. H., and Chung, A. S. (2003) Roles of matrix metalloproteinases in tumor metastasis and angiogenesis. *J Biochem Mol Biol* 36, 128-137.

28. Liao, S. H., Zhao, X. Y., Han, Y. H., Zhang, J., Wang, L. S., Xia, L., Zhao, K. W., Zheng, Y., Guo, M., and Chen, G. Q. (2009) Proteomics-based identification of two novel direct targets of hypoxia-inducible factor-1 and their potential roles in migration/invasion of cancer cells. *Proteomics* 9, 3901-3912.

29. Arimoto-Ishida, E., Sakata, M., Sawada, K., Nakayama, M., Nishimoto, F., Mabuchi, S., Takeda, T., Yamamoto, T., Isobe, A., Okamoto, Y., Lengyel, E., Suehara, N., Morishige, K., and Kimura, T. (2009) Up-regulation of alpha5-integrin by E-cadherin loss in hypoxia and its key role in the migration of extravillous trophoblast cells during early implantation. *Endocrinology* 150, 4306-4315.

30. Kim, S. H., Xia, D., Kim, S. W., Holla, V., Menter, D. G., and Dubois, R. N. (2010) Human enhancer of filamentation 1 Is a mediator of hypoxia-inducible factor-1alpha-mediated migration in colorectal carcinoma cells. *Cancer Res* 70, 4054-4063.

31. Kuonen, F., Secondini, C., and Ruegg, C. (2012) Molecular Pathways: Emerging pathways mediating growth, invasion and metastasis of tumors progressing in an irradiated microenvironment. *Clin Cancer Res*.

32. Stockwin, L. H., Blonder, J., Bumke, M. A., Lucas, D. A., Chan, K. C., Conrads, T. P., Issaq, H. J., Veenstra, T. D., Newton, D. L., and Rybak, S. M. (2006) Proteomic analysis of plasma membrane from hypoxia-adapted malignant melanoma. *J Proteome Res* 5, 2996-3007.

33. Sorensen, B. S., Horsman, M. R., Vorum, H., Honore, B., Overgaard, J., and Alsner, J. (2009) Proteins upregulated by mild and severe hypoxia in squamous cell carcinomas in vitro identified by proteomics. *Radiother Oncol* 92, 443-449.

34. Vorum, H., Ostergaard, M., Hensechke, P., Enghild, J. J., Riazati, M., and Rice, G. E. (2004) Proteomic analysis of hyperoxia-induced responses in the human choriocarcinoma cell line JEG-3. *Proteomics* 4, 861-867.

35. Kumar, G. K., and Klein, J. B. (2004) Analysis of expression and posttranslational modification of proteins during hypoxia. *J Appl Physiol* 96, 1178-1186; discussion 1170-1172.

36. Dettmer, K., Nurnberger, N., Kaspar, H., Gruber, M. A., Almstetter, M. F., and Oefner, P. J. (2011) Metabolite extraction from adherently growing mammalian cells for metabolomics studies: optimization of harvesting and extraction protocols. *Anal Bioanal Chem* 399, 1127-1139.

37. Finley, L. W., Carracedo, A., Lee, J., Souza, A., Egia, A., Zhang, J., Teruya-Feldstein, J., Moreira, P. I., Cardoso, S. M., Clish, C. B., Pandolfi, P. P., and Haigis, M. C. (2011) SIRT3 opposes reprogramming of cancer cell metabolism through HIF1alpha destabilization. *Cancer Cell* 19, 416-428.

38. Lara, P. C., Lloret, M., Clavo, B., Apolinario, R. M., Bordon, E., Rey, A., Falcon, O., Alonso, A. R., and Belka, C. (2008) Hypoxia downregulates Ku70/80 expression in cervical carcinoma tumors. *Radiother Oncol* 89, 222-226.

39. Chen, D. J., and Nirodi, C. S. (2007) The epidermal growth factor receptor: a role in repair of radiation-induced DNA damage. *Clin Cancer Res* 13, 6555-6560.

40. Ting, N. S., Chan, D. W., Lintott, L. G., Allalunis-Turner, J., and Lees-Miller, S. P. (1999) Protein-DNA complexes containing DNA-dependent protein kinase in crude extracts from human and rodent cells. *Radiat Res* 151, 414-422.

41. Lou, Z., Chen, B. P., Asaithamby, A., Minter-Dykhouse, K., Chen, D. J., and Chen, J. (2004) MDC1 regulates DNA-PK autophosphorylation in response to DNA damage. *J Biol Chem* 279, 46359-46362.

42. Salton, M., Lerenthal, Y., Wang, S. Y., Chen, D. J., and Shiloh, Y. (2010) Involvement of Matrin 3 and SFPQ/NONO in the DNA damage response. *Cell Cycle* 9, 1568-1576.

43. Kumari, A., Mazina, O. M., Shinde, U., Mazin, A. V., and Lu, H. (2009) A role for SSRP1 in recombination-mediated DNA damage response. *J Cell Biochem* 108, 508-518.

44. Li, Y., Bolderson, E., Kumar, R., Muniandy, P. A., Xue, Y., Richard, D. J., Seidman, M., Pandita, T. K., Khanna, K. K., and Wang, W. (2009) HSSB1 and hSSB2 form similar multiprotein complexes that participate in DNA damage response. *J Biol Chem* 284, 23525-23531.

45. Clements, P. M., Breslin, C., Deeks, E. D., Byrd, P. J., Ju, L., Bieganowski, P., Brenner, C., Moreira, M. C., Taylor, A. M., and Caldecott, K. W. (2004) The ataxia-oculomotor apraxia 1 gene product has a role distinct from ATM and interacts with the DNA strand break repair proteins XRCC1 and XRCC4. *DNA Repair (Amst)* 3, 1493-1502.

46. Mahajan, K. N., and Mitchell, B. S. (2003) Role of human Pso4 in mammalian DNA repair and association with terminal deoxynucleotidyl transferase. *Proc Natl Acad Sci U S A* 100, 10746-10751.

47. Boros, L. G., Lee, W. N., and Go, V. L. (2002) A metabolic hypothesis of cell growth and death in pancreatic cancer. *Pancreas* 24, 26-33.

48. Chen, C., Pore, N., Behrooz, A., Ismail-Beigi, F., and Maity, A. (2001) Regulation of glut1 mRNA by hypoxia-inducible factor-1. Interaction between H-ras and hypoxia. *J Biol Chem* 276, 9519-9525.

49. Mikuriya, K., Kuramitsu, Y., Ryozawa, S., Fujimoto, M., Mori, S., Oka, M., Hamano, K., Okita, K., Sakaida, I., and Nakamura, K. (2007) Expression of glycolytic enzymes is increased in pancreatic cancerous tissues as evidenced by proteomic profiling by two-dimensional electrophoresis and liquid chromatography-mass spectrometry/mass spectrometry. *Int J Oncol* 30, 849-855.

50. Cai, Z., Zhao, J. S., Li, J. J., Peng, D. N., Wang, X. Y., Chen, T. L., Qiu, Y. P., Chen, P. P., Li, W. J., Xu, L. Y., Li, E. M., Tam, J. P., Qi, R. Z., Jia, W., and Xie, D. (2010) A combined proteomics and metabolomics profiling of gastric cardia cancer reveals characteristic dysregulations in glucose metabolism. *Mol Cell Proteomics* 9, 2617-2628.

51. Izumi, H., Takahashi, M., Uramoto, H., Nakayama, Y., Oyama, T., Wang, K. Y., Sasaguri, Y., Nishizawa, S., and Kohno, K. (2011) Monocarboxylate transporters 1 and 4 are involved in the invasion activity of human lung cancer cells. *Cancer Sci* 102, 1007-1013.

52. Fan, J., Zhou, J. Q., Yu, G. R., and Lu, D. D. (2010) Glucose transporter protein 1-targeted RNA interference inhibits growth and invasion of the osteosarcoma cell line MG63 in vitro. *Cancer Biother Radiopharm* 25, 521-527.

53. Maschek, G., Savaraj, N., Priebe, W., Braunschweiger, P., Hamilton, K., Tidmarsh, G. F., De Young, L. R., and Lampidis, T. J. (2004) 2-deoxy-D-glucose increases the efficacy of adriamycin and paclitaxel in human osteosarcoma and non-small cell lung cancers in vivo. *Cancer Res* 64, 31-34.

54. Zhong, D., Xiong, L., Liu, T., Liu, X., Chen, J., Sun, S. Y., Khuri, F. R., Zong, Y., Zhou, Q., and Zhou, W. (2009) The glycolytic inhibitor 2-deoxyglucose activates multiple prosurvival pathways through IGF1R. *J Biol Chem* 284, 23225-23233.

55. Gilcrease, M. Z., Truong, L., and Brown, R. W. (1996) Correlation of very late activation integrin and CD44 expression with extrarenal invasion and metastasis of renal cell carcinomas. *Hum Pathol* 27, 1355-1360.

56. Hynes, R. O. (2002) Integrins: bidirectional, allosteric signaling machines. *Cell* 110, 673-687.

57. Chammas, R., and Brentani, R. (1991) Integrins and metastases: an overview. *Tumour Biol* 12, 309-320.

58. Janik, M. E., Litynska, A., and Vereecken, P. (2010) Cell migration-the role of integrin glycosylation. *Biochim Biophys Acta* 1800, 545-555.

59. Leitinger, B., and Hohenester, E. (2007) Mammalian collagen receptors. *Matrix Biol* 26, 146-155.

60. Ryu, M. H., Park, H. M., Chung, J., Lee, C. H., and Park, H. R. (2010) Hypoxia-inducible factor-1alpha mediates oral squamous cell carcinoma invasion via upregulation of alpha5 integrin and fibronectin. *Biochem Biophys Res Commun* 393, 11-15.

61. Hogg, N., and Landis, R. C. (1993) Adhesion molecules in cell interactions. *Curr Opin Immunol* 5, 383-390.

62. Fitsialos, G., Bourget, I., Augier, S., Ginouves, A., Rezzonico, R., Odorisio, T., Cianfarani, F., Virolle, T., Pouyssegur, J., Meneguzzi, G., Berra, E., Ponzio, G., and Busca, R. (2008) HIF1 transcription factor regulates laminin-332 expression and keratinocyte migration. *J Cell Sci* 121, 2992-3001.

63. Kajimoto, T., and Node, M. (2009) Inhibitors against glycosidases as medicines. *Curr Top Med Chem* 9, 13-33.

64. Elbein, A. D. (1991) Glycosidase inhibitors: inhibitors of N-linked oligosaccharide processing. *Faseb J* 5, 3055-3063.

65. Kornfeld, R., and Kornfeld, S. (1985) Assembly of asparagine-linked oligosaccharides. *Annu Rev Biochem* 54, 631-664.

66. Zhao, Y., Liu, W., Zhou, Y., Zhang, X., and Murphy, P. V. (2010) N-(8-(3-ethynylphenoxy)octyl-1-deoxynojirimycin suppresses growth and migration of human lung cancer cells. *Bioorg Med Chem Lett* 20, 7540-7543.

67. Shuai, K., Schindler, C., Prezioso, V. R., and Darnell, J. E., Jr. (1992) Activation of transcription by IFN-gamma: tyrosine phosphorylation of a 91-kD DNA binding protein. *Science* 258, 1808-1812.

68. Schindler, C., Levy, D. E., and Decker, T. (2007) JAK-STAT signaling: from interferons to cytokines. *J Biol Chem* 282, 20059-20063.

69. Khodarev, N. N., Roach, P., Pitroda, S. P., Golden, D. W., Bhayani, M., Shao, M. Y., Darga, T. E., Beveridge, M. G., Sood, R. F., Sutton, H. G., Beckett, M. A., Mauceri, H. J., Posner, M. C., and Weichselbaum, R. R. (2009) STAT1 pathway mediates amplification of metastatic potential and resistance to therapy. *PLoS One* 4, e5821.

70. Wen, Z., Zhong, Z., and Darnell, J. E., Jr. (1995) Maximal activation of transcription by Stat1 and Stat3 requires both tyrosine and serine phosphorylation. *Cell* 82, 241-250.

71. Decker, T., and Kovarik, P. (2000) Serine phosphorylation of STATs. *Oncogene* 19, 2628-2637.

72. Ouchi, T., Lee, S. W., Ouchi, M., Aaronson, S. A., and Horvath, C. M. (2000) Collaboration of signal transducer and activator of transcription 1 (STAT1) and BRCA1 in differential regulation of IFN-gamma target genes. *Proc Natl Acad Sci U S A* 97, 5208-5213.

73. Zhang, J. J., Zhao, Y., Chait, B. T., Lathem, W. W., Ritzi, M., Knippers, R., and Darnell, J. E., Jr. (1998) Ser727-dependent recruitment of MCM5 by Stat1alpha in IFN-gamma-induced transcriptional activation. *Embo J* 17, 6963-6971.

74. Pine, R. (1997) Convergence of TNFalpha and IFNgamma signalling pathways through synergistic induction of IRF-1/ISGF-2 is mediated by a composite GAS/kappaB promoter element. *Nucleic Acids Res* 25, 4346-4354.

75. Mamane, Y., Heylbroeck, C., Genin, P., Algarte, M., Servant, M. J., LePage, C., DeLuca, C., Kwon, H., Lin, R., and Hiscott, J. (1999) Interferon regulatory factors: the next generation. *Gene* 237, 1-14.

76. Liu, B., Liao, J., Rao, X., Kushner, S. A., Chung, C. D., Chang, D. D., and Shuai, K. (1998) Inhibition of Stat1-mediated gene activation by PIAS1. *Proc Natl Acad Sci U S A* 95, 10626-10631.

77. Lee, M. Y., Joung, Y. H., Lim, E. J., Park, J. H., Ye, S. K., Park, T., Zhang, Z., Park, D. K., Lee, K. J., and Yang, Y. M. (2006) Phosphorylation and activation of STAT proteins by hypoxia in breast cancer cells. *Breast* 15, 187-195.

78. Terui, K., Haga, S., Enosawa, S., Ohnuma, N., and Ozaki, M. (2004) Hypoxia/re-oxygenation-induced, redox-dependent activation of STAT1 (signal transducer and activator of transcription 1) confers resistance to apoptotic cell death via hsp70 induction. *Biochem J* 380, 203-209.

79. Stephanou, A., Brar, B. K., Scarabelli, T. M., Jonassen, A. K., Yellon, D. M., Marber, M. S., Knight, R. A., and Latchman, D. S. (2000) Ischemia-induced STAT-1 expression and activation play a critical role in cardiomyocyte apoptosis. *J Biol Chem* 275, 10002-10008.

80. Stephanou, A. (2002) Activated STAT-1 pathway in the myocardium as a novel therapeutic target in ischaemia/reperfusion injury. *Eur Cytokine Netw* 13, 401-403.

81. Ivanov, S. V., Salnikow, K., Ivanova, A. V., Bai, L., and Lerman, M. I. (2007) Hypoxic repression of STAT1 and its downstream genes by a pVHL/HIF-1 target DEC1/STRA13. *Oncogene* 26, 802-812.

82. Chin, Y. E., Kitagawa, M., Su, W. C., You, Z. H., Iwamoto, Y., and Fu, X. Y. (1996) Cell growth arrest and induction of cyclin-dependent kinase inhibitor p21 WAF1/CIP1 mediated by STAT1. *Science* 272, 719-722.

83. Chin, Y. E., Kitagawa, M., Kuida, K., Flavell, R. A., and Fu, X. Y. (1997) Activation of the STAT signaling pathway can cause expression of caspase 1 and apoptosis. *Mol Cell Biol* 17, 5328-5337.

84. Bromberg, J. F., Fan, Z., Brown, C., Mendelsohn, J., and Darnell, J. E., Jr. (1998) Epidermal growth factor-induced growth inhibition requires Stat1 activation. *Cell Growth Differ* 9, 505-512.

85. Taniguchi, T. (1997) Transcription factors IRF-1 and IRF-2: linking the immune responses and tumor suppression. *J Cell Physiol* 173, 128-130.

86. Lee, K. Y., Anderson, E., Madani, K., and Rosen, G. D. (1999) Loss of STAT1 expression confers resistance to IFN-gamma-induced apoptosis in ME180 cells. *FEBS Lett* 459, 323-326.

87. Hiroi, M., Mori, K., Sakaeda, Y., Shimada, J., and Ohmori, Y. (2009) STAT1 represses hypoxia-inducible factor-1-mediated transcription. *Biochem Biophys Res Commun* 387, 806-810.

88. Huang, S., Bucana, C. D., Van Arsdall, M., and Fidler, I. J. (2002) Stat1 negatively regulates angiogenesis, tumorigenicity and metastasis of tumor cells. *Oncogene* 21, 2504-2512.

89. Hu, Y., Hu, X., Boumsell, L., and Ivashkiv, L. B. (2008) IFN-gamma and STAT1 arrest monocyte migration and modulate RAC/CDC42 pathways. *J Immunol* 180, 8057-8065.

90. Dutreix, M., Cosset, J. M., and Sun, J. S. (2010) Molecular therapy in support to radiotherapy. *Mutat Res* 704, 182-189.

91. Kim, Y. J., and Varki, A. (1997) Perspectives on the significance of altered glycosylation of glycoproteins in cancer. *Glycoconj J* 14, 569-576.

List of Figures

DJ for 48h first to suppress glycoprotein synthesis, Magnification, x100; D, The inhibition of glycoprotein synthesis after 1-DJ treatment was verified in lectin binding assay by WB; E, The effect of 1-DJ in inhibition of cell migration at 100μM concentration.

Fig.5, Confirmation of STAT1 pathway suppressed by hypoxia and validation of stable cell lines with STAT1a overexpression in A431; A, Change patterns of STAT1 and its downstream proteins due to hypoxia or reoxygenation; B, The down-regulation of STAT1 and pSTAT1a (S727) was confirmed by WB. C, The decrease of functional STAT1 represses the transcription of its downstream genes. D, The two positive stable cell lines with STAT1a overexpression were confirmed by WB using anti-FLAG, STAT1 and pSTAT1a (S727) antibodies. E, The activation of downstream genes of STAT1 in the stable cell lines indicated that the cell lines indeed have more active STAT1a.

Fig.6, Overexpression of STAT1a suppresses the migration and enhances the adhesion of A431. A, MTT assay under Nx and Hx; B and C, Images and quantification of scratch assay of control and STAT1a overexpression A431 cells, Magnification, x100; D and E, Images and quantification of adhesion assay of control and STAT1 overexpression A431 cells.

List of Tables

Table 1. Data analysis of identified proteins modulated by hypoxia

	115:114	116:114	117:114	Unique protein No.	Total
P<0.05	1281	1260	1035	1904*	
Ratio>1.2	334	255	203	522**	1253#
Ratio<0.83	560	398	288	743***	

*The number of unique proteins with at least one ratio with p<0.05

** The number of unique proteins up-regulated with p<0.05

*** The number of unique proteins down-regulated with p<0.05

The number of unique proteins with significant change under hypoxia or reoxygenation

Fig. 1

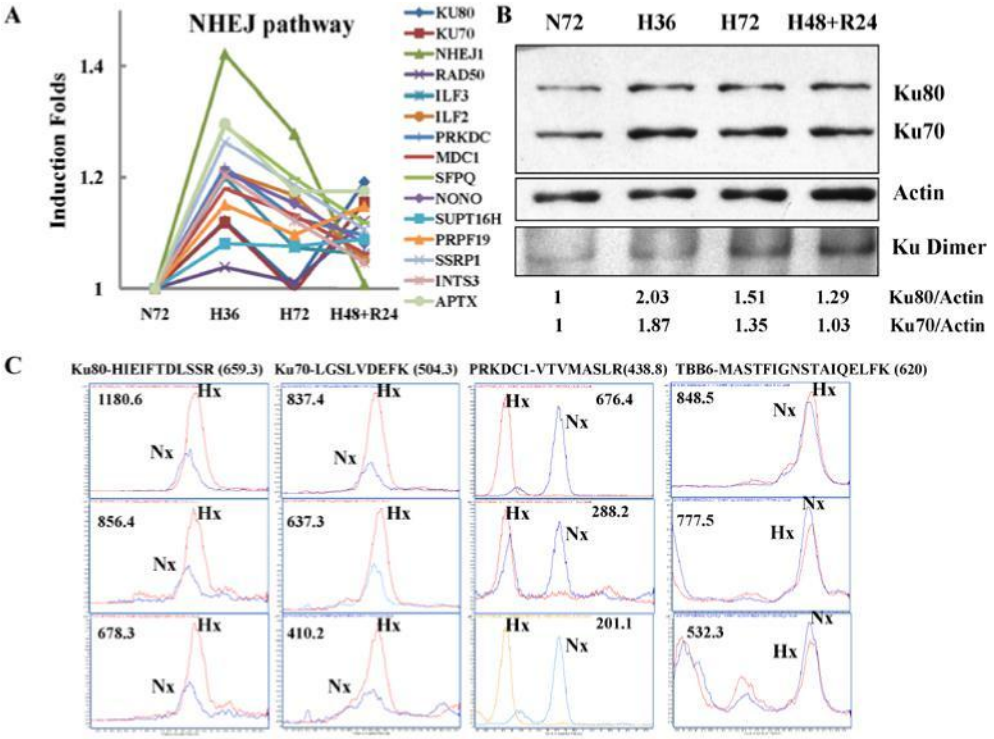
A
NHEJ pathway
Induction Folds
1.4
1.2
1
N72
H36
H72
H48+R24
KU80
KU70
NHEJ1
RAD50
ILF3
ILF2
PRKDC
MDC1
SFPQ
NONO
SUPT16H
PRPF19
SSRP1
INTS3
APTX
B
N72
H36
H72
H48+R24
Ku80
Ku70
Actin
Ku Dimer
1 2.03 1.51 1.29 Ku80/Actin
1 1.87 1.35 1.03 Ku70/Actin
C
Ku80-HIEIFTDLSSR (659.3)
Ku70-LGSLVDEFK (504.3)
PRKDC1-VTVMASLR(438.8)
TBB6-MASTFIGNSTAIQELFK (620)
1180.6
837.4
676.4
848.5
856.4
637.3
288.2
777.5
678.3
410.2
201.1
532.3
Hx
Nx

Fig. 2

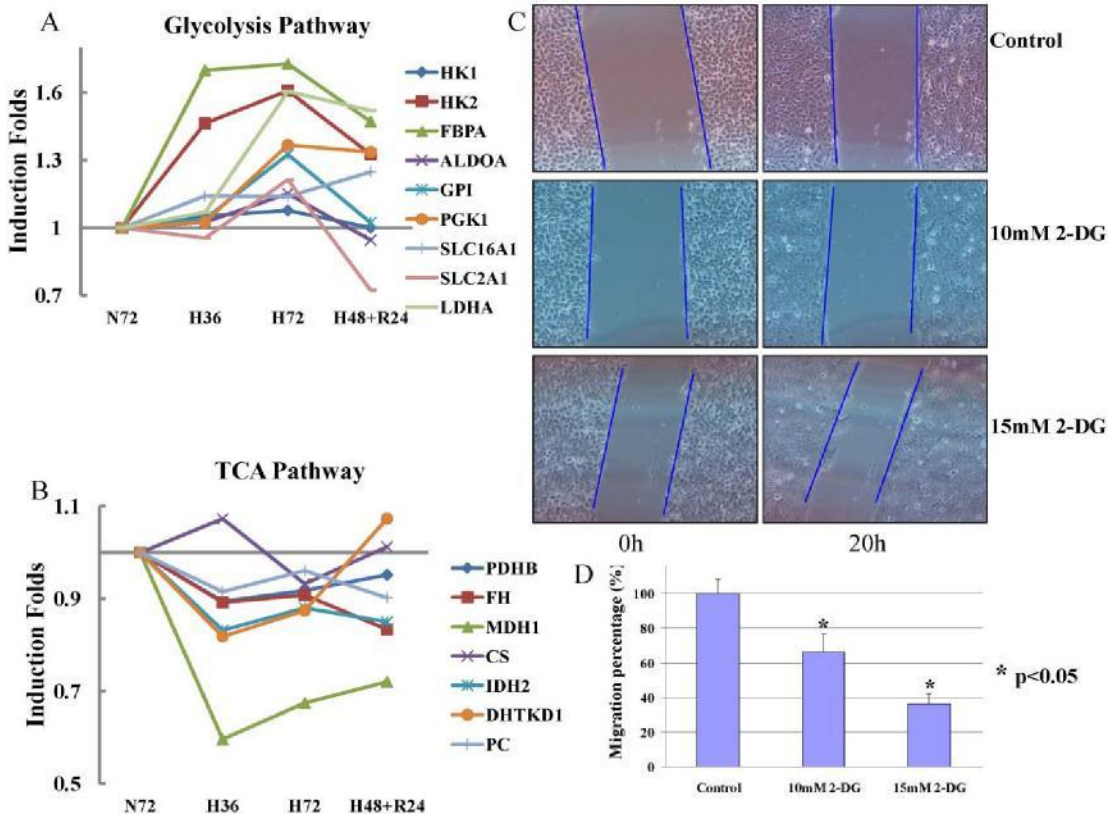
A
Glycolysis Pathway
Induction Folds
1.6
1.3
1
0.7
N72
H36
H72
H48+R24
HK1
HK2
FBPA
ALDOA
GPI
PGK1
SLC16A1
SLC2A1
LDHA
B
TCA Pathway
Induction Folds
1.1
0.9
0.7
0.5
N72
H36
H72
H48+R24
PDHB
FH
MDH1
CS
IDH2
DHTKD1
PC
C
Control
10mM 2-DG
15mM 2-DG
0h
20h
D
Migration percentage (%)
100
80
60
40
20
0
Control
10mM 2-DG
15mM 2-DG
* p<0.05

Fig. 3

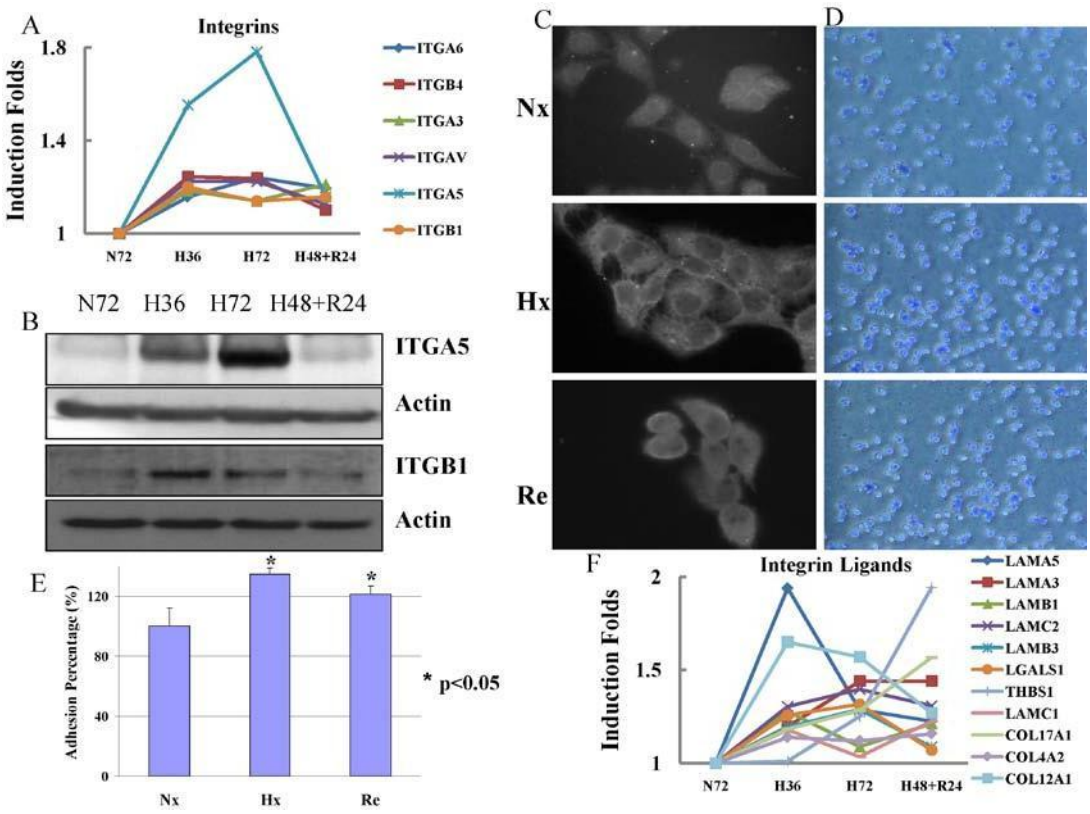
A
Integrins
Induction Folds
1.8
1.4
1
N72
H36
H72
H48+R24
ITGA6
ITGB4
ITGA3
ITGAV
ITGA5
ITGB1
B
N72 H36 H72 H48+R24
ITGA5
Actin
ITGB1
Actin
C
D
Nx
Hx
Re
E
Adhesion Percentage (%)
120
80
40
0
Nx
Hx
Re
* p<0.05
F
Integrin Ligands
Induction Folds
2
1.5
1
N72
H36
H72
H48+R24
LAMA5
LAMA3
LAMB1
LAMC2
LAMB3
LGALS1
THBS1
LAMC1
COL17A1
COL4A2
COL12A1

Fig. 4

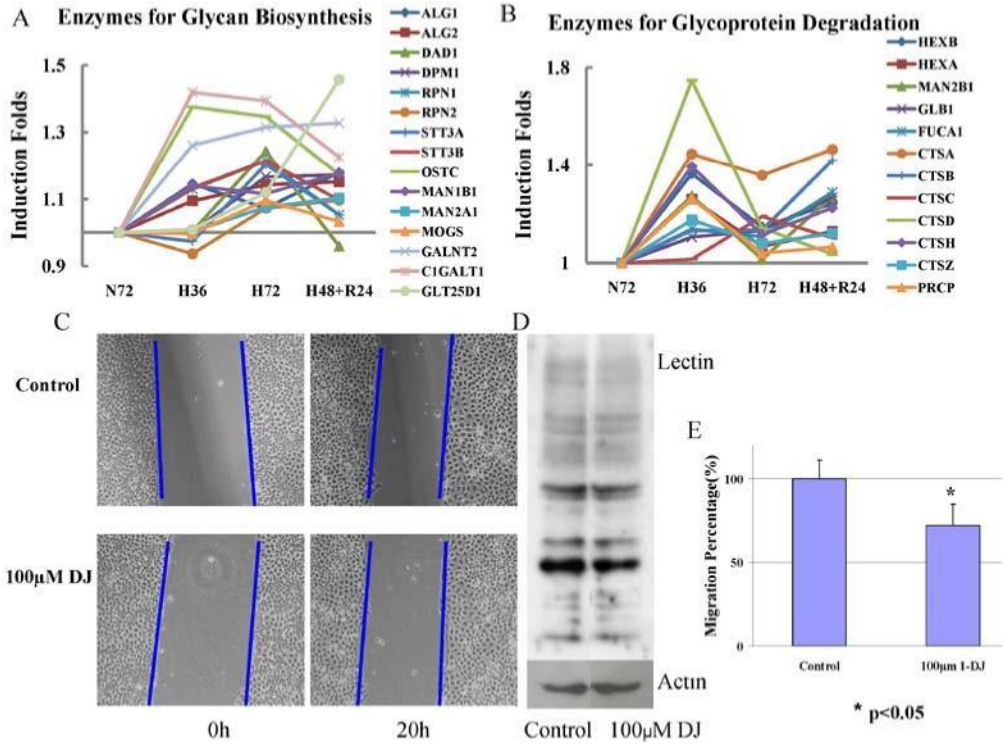
A
Enzymes for Glycan Biosynthesis
Induction Folds
1.5
1.3
1.1
0.9
N72
H36
H72
H48+R24
ALG1
ALG2
DAD1
DPM1
RPN1
RPN2
STT3A
STT3B
OSTC
MAN1B1
MAN2A1
MOGS
GALNT2
C1GALT1
GLT25D1
B
Enzymes for Glycoprotein Degradation
Induction Folds
1.8
1.4
1
N72
H36
H72
H48+R24
HEXB
HEXA
MAN2B1
GLB1
FUCA1
CTSA
CTSB
CTSC
CTSD
CTSH
CTSZ
PRCP
C
Control
100μM DJ
0h
20h
D
Lectin
Actin
Control
100μM DJ
E
Migration Percentage(%)
100
50
0
Control
100μm 1-DJ
*
* p<0.05

Fig. 5

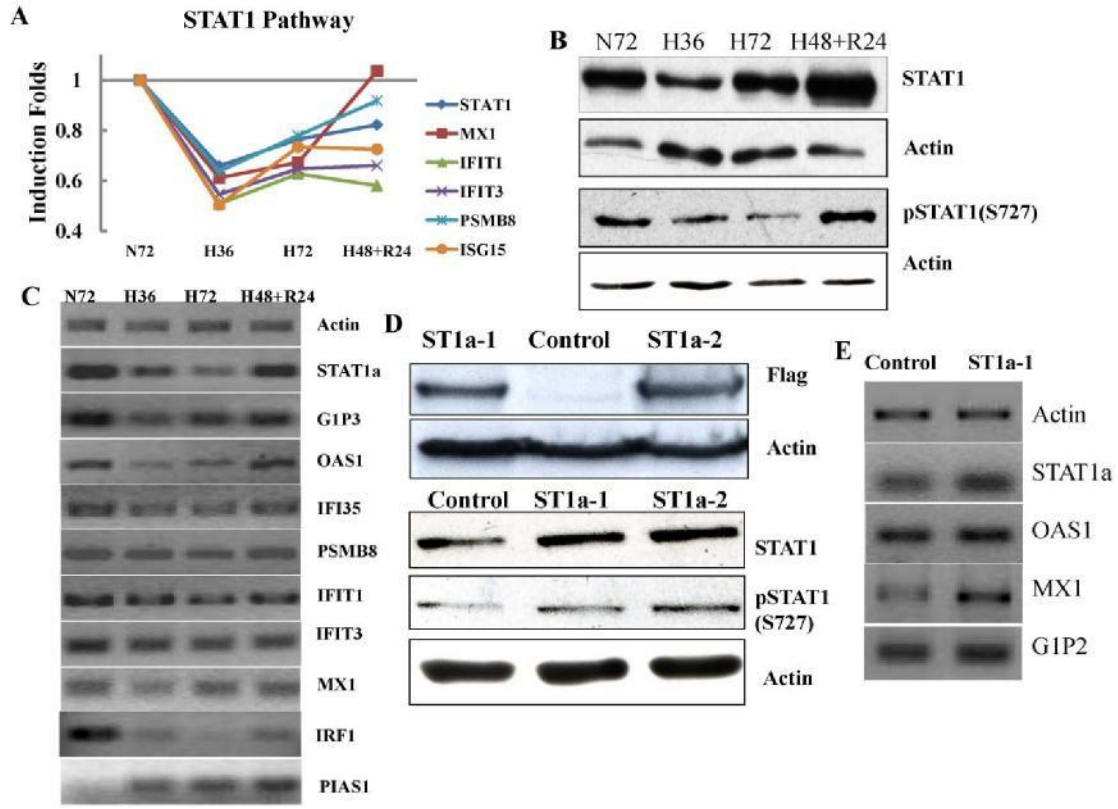
A
STAT1 Pathway
Induction Folds
1
0.8
0.6
0.4
N72
H36
H72
H48+R24
STAT1
MX1
IFIT1
IFIT3
PSMB8
ISG15
B
N72
H36
H72
H48+R24
STAT1
Actin
pSTAT1(S727)
Actin
C
N72
H36
H72
H48+R24
Actin
STAT1a
G1P3
OAS1
IFI35
PSMB8
IFIT1
IFIT3
MX1
IRF1
PIAS1
D
ST1a-1
Control
ST1a-2
Flag
Actin
Control
ST1a-1
ST1a-2
STAT1
pSTAT1 (S727)
Actin
E
Control
ST1a-1
Actin
STAT1a
OAS1
MX1
G1P2

Fig. 6

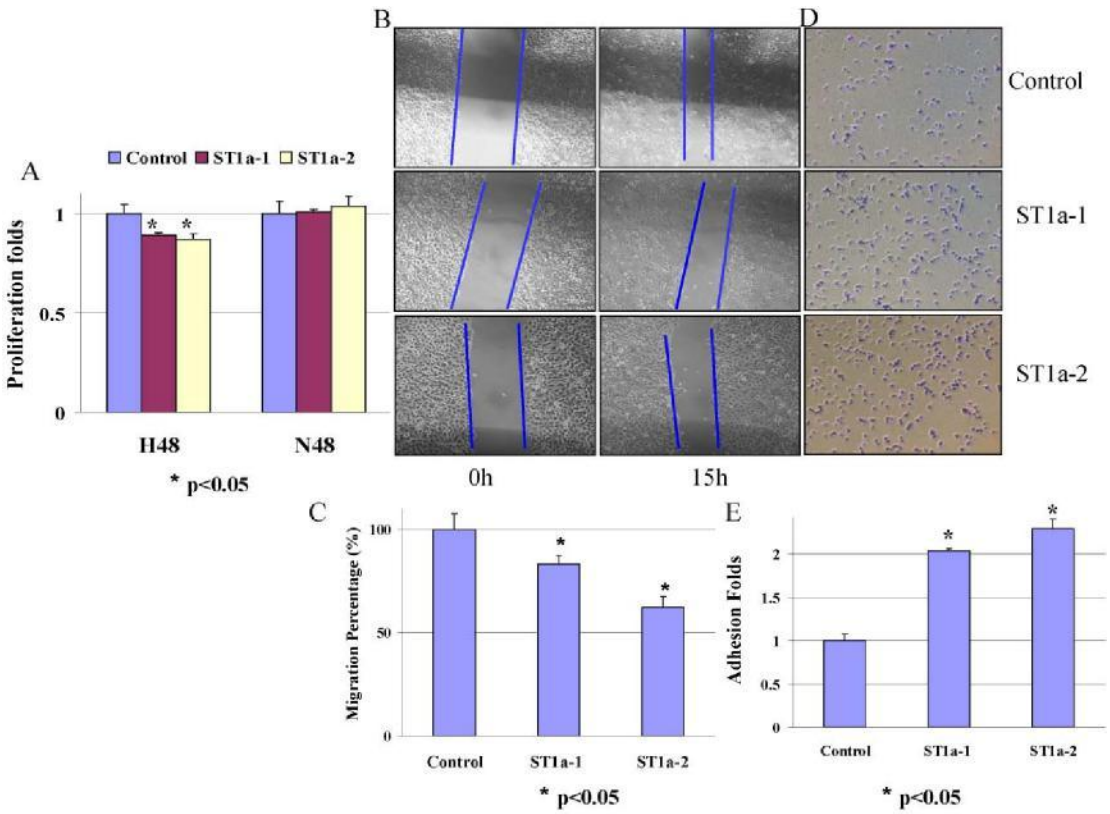
A
Control
ST1a-1
ST1a-2
Proliferation folds
1
0.5
0
H48
N48
* p<0.05
B
0h
15h
D
Control
ST1a-1
ST1a-2
C
Migration Percentage (%)
100
50
0
Control
ST1a-1
ST1a-2
* p<0.05
E
Adhesion Folds
2
1.5
1
0.5
0
Control
ST1a-1
ST1a-2
* p<0.05